Chemical Engineering Journal 96 (2003) 133–143

Chemical Engineering Journal

www.elsevier.com/locate/cej

Theoretical analysis of the flow regimes and their characteristics in vertically flowing gas–solids suspensions

Y. Molodtsof*

Département de Génie Chimique, Université de Technologie de Compiègne, UMR 6067, BP 20529, 60205 Compiegne, France

Abstract

This paper analyses the detailed flow structure characteristics of a vertical, fully developed gas–solids suspension. It is based on an asymptotic approach to general multiphase flow equations, in the range of low or moderate solids concentrations. Three distinct flow structures are identified, defining the Similar Profiles, Transition and Dense Phase Flow Regimes, as well as the local mechanism generating the transitions. The predicted properties of the trends of variation of local flow variables, with overall solids loading are, then, compared with existing experimental data. The observed wide agreement encourages the use of the theory for the interpretation and the prediction of the behavior of existing industrial units.

Keywords: Flow regimes; Gas–solids suspensions; Multiphase flow equations; Flow structure; Circulating fluidized bed

1. Introduction

The vertical flow of gas–solids suspensions is relevant for many industrial applications such as pneumatic transport, Circulating Fluidized Bed (CFB) or Downer reactors. Especially for the operation of chemical reactors, the hydrodynamic characteristics of the flow are of crucial importance since, the coming into contact of the phases which controls reaction rate is completely dependent on the flow structure of the gas–solids mixture. The flow structure, in turn, is determined by the operating variables of the installation. Therefore, the relationship between operating variables and the resulting flow structure is a central requirement for proper plant operation.

Besides, the flow regime concept is more or less implicitly associated with an identified flow structure, the characteristics of which remain invariant over a more or less wide range of operating parameters. Consequently, there is a long lasting concern for predicting fluidization regimes and classifying them in terms of particle properties and operating parameter ranges. This preoccupation is traceable through scientific and technical literature, with several regime diagrams published, e.g., by Zenz [1], Reh [2], Yerushalmi et al. [3], Matsen [4], Grace [5], Mok et al. [6,7]. Unlike the latter, the first five diagrams allow the determination of the conditions under which a given gas–particle system can be expected to provide, e.g., a CFB-type flow regime. On the contrary, Mok attempted a classification of CFB-type flow regimes in terms of gas velocity and particle loading ranges, for a given gas–solids system and a given installation.

Thus, the prediction of flow regimes also requires the preliminary identification of the relevant operating variables, which determine the flow characteristics. Especially for the CFB, which has been approached either through high velocity fluidization or pneumatic transport, the question required clarification. In a recent paper Berruti et al. [8] examined the effect of the operating principle of each particular CFB installation on the hydrodynamic characteristics of the flow in the riser. They distinguished between Variable Inventory Systems (VIS) and Fixed Inventory Systems (FIS). Roughly speaking, in the latter case, the overall solids inventory is an operating variable of the process, together with gas velocity, while, in VIS-type operation, the operating parameters are gas velocity and solids circulation rate (or, solids loading of riser flow).

This work is devoted to a detailed theoretical analysis of the flow structures and flow regimes expected to occur in a vertical, fully developed suspension flow, at a constant gas superficial velocity, when the solids loading is varied, regardless of the means (varying solids inventory or, circulation rate) used to adjust solids concentration. Fully developed flow and its characteristics are relevant for constant cross-section risers or downers and even, for their flow development sections, as it has been recently illustrated by Motte [9].

* Tel.: +33-3-44-23-4434; fax: +33-3-44-23-1980.
E-mail address: yuri.molodtsof@utc.fr (Y. Molodtsof).

1385-8947/$ – see front matter © 2003 Elsevier B.V. All rights reserved.
doi:10.1016/j.cej.2003.08.014

Nomenclature

A	cross-sectional area of the riser (m^2)
B_{ij}	gas velocity cofluctuations tensor (m^2/s^2)
F	gas–solids interaction force (N/m^3)
g	acceleration of gravity (m/s^2)
p	local gas pressure
r	radial distance to riser centerline (m)
s_{ij}	intergranular stress tensor (Pa)
U	gas velocity (m/s)
V	solids velocity (m/s)
x	axial coordinate (m)

Greek letters

α	phase presence probability (–)
β_{ij}	solids velocity cofluctuations tensor (m^2/s^2)
ϕ_s	solids axial mass flux (kg/m^2 s)
ρ	phase density (kg/m^3)
σ_{ij}	solids stress tensor (Pa)
τ_{ij}	gas viscous stress tensor (Pa)

Subscripts and superscripts

D	Dense Phase Flow Regime
f	the fluid phase
i, j	tensor notation
K	interval K
R	reference flow variables
s	the solids phase
T	the Transition Regime
$\bar{X}$	(overbar) indicates cross-sectional averages
*	critical conditions
0	unladen gas flow variables
1	the Similar Profiles Regime

The analysis is based on an asymptotic approach of the General equations governing the flow of gas–solids mixtures [10,11], following the method initiated in a previous paper [10,12]. Its main objective is to provide a rigorous theoretical background to a series of experimental investigations, which already identified flow regimes and flow structure characteristics, in order to be able to interpret and generalize experimental findings. For this purpose, a general discussion of these findings with the help of theoretical results will take place in the last section of the paper.

2. General analysis

2.1. General equations for fully developed flow

General probabilistic multiphase flow equations [10,11] provide a rigorous basis for the analysis of gas–solids flow. They have been derived from first principles, taking into account the intrinsic stochastic nature of the flow of multiphase mixtures, and using an ensemble averaging technique. These Eulerian equations are labeled in terms of local and instantaneous *phase mean variables* defined as the probabilistic means (i.e., expected values) of the immediate Eulerian variables of each phase. An equivalence theorem enables the direct identification of each phase mean variable with the corresponding physically measurable quantity.

For a gas–solids mixture, when all the particles making up the solids exhibit the same density, the flow can be considered as a two-phase flow [11] which is governed by two Continuity Equations (one for each phase) and six Momentum Equations. In the case of a fully developed flow of a gas–solids suspension in a circular pipe, it can be shown, with the help of the Continuity Equations, that the velocity fields are strictly axial for each phase [10,11]. In addition, all the variables in the Momentum Equations, except pressure, only depend upon the radial coordinate r. Consequently, for the fluid phase, for instance, the axial projection of the Momentum Equation simplifies as follows:

$$\frac{1}{r}\frac{\mathrm{d}}{\mathrm{d}r}(r\alpha_\mathrm{f}\rho_\mathrm{f}B_{rx}) = -\alpha_\mathrm{f}\rho_\mathrm{f}g - \alpha_\mathrm{f}\frac{\partial p}{\partial x} - F_x + \frac{1}{r}\frac{\mathrm{d}}{\mathrm{d}r}(r\alpha_\mathrm{f}\tau_{rx}) \tag{1}$$

The LHS of this equation contains the remainder of the inertia forces, where, B_{rx} denotes shear component of the velocity cofluctuations tensor ($-\rho B_{ij}$ identifies with Reynolds turbulent stresses in one-phase fluid flow). The RHS accounts for the external forces, respectively, gravity, pressure forces, gas–solids interaction (F_x) and viscous stresses (τ_{rx}). Finally, α_f denotes the local probability of presence of the fluid.

The analogous equation for the solids, simplifies as follows:

$$\frac{1}{r}\frac{\mathrm{d}}{\mathrm{d}r}(r\alpha_\mathrm{s}\rho_\mathrm{s}\beta_{rx}) = -\alpha_\mathrm{s}\rho_\mathrm{s}g - \alpha_\mathrm{s}\frac{\partial p}{\partial x} + F_x + \frac{1}{r}\frac{\mathrm{d}}{\mathrm{d}r}[r(\alpha_\mathrm{s}\sigma_{rx} + s_{rx})] \tag{2}$$

Most of the terms in this equation are similar to corresponding ones in Eq. (1). Two particularities, however, should be noted. The effect of average gas pressure on particles takes the particular form shown here, only in the case of a fully developed flow [10]. Besides, the last term, in the RHS of Eq. (2) exhibits two different stress tensors; σ_{rx} accounts for surface forces acting continuously in time and linked by the fluid, while, s_{rx} generally known as the intergranular stress, contains the effect of direct contacts (here, mainly collisions) with other surfaces, i.e., particles and walls.

In addition to the axial pressure gradient and the gas–solids interaction force, these two equations are coupled by the phases complementarity equation:

$$\alpha_\mathrm{f} + \alpha_\mathrm{s} = 1 \tag{3}$$

where α_s represents the local solids presence probability, which can be identified with solids volumetric concentration (i.e., solids volume fraction).

Simplifications introduced in the General equations in order to derive Eqs. (1) and (2) are only based on the fully developed flow hypothesis and, therefore, are completely rigorous. However, there is an obvious closure problem related with these equations. Indeed, these equations cannot be solved until additional equations are derived in order to express B_{rx}, β_{rx}, F_x, τ_{rx}, σ_{rx} and s_{rx} in terms of basic variables such as phases velocities and concentrations. Rigorously modeling so many terms to derive the required number of closure equations will probably not be possible for several decades, despite numerous attempts which can already be found in literature (e.g. [13,14]). In order to avoid this closure problem, solving Eqs. (1)–(3) will not be attempted in this work. Rather, the previously developed asymptotic approach [12] will be used to analyze the flow structure problem.

Finally, the analysis to be developed hereafter is an asymptotic one, limited to the cases where the average solids concentration remains low. This average concentration is defined as the cross-sectional average of α_s:

$$\bar{\alpha}_s = \frac{1}{A}\int_A \alpha_s \, dA \tag{4}$$

Adding through Eqs. (1) and (2) eliminates the gas–solids interaction force F_x. Then, using Eq. (3), one obtains

$$\frac{1}{r}\frac{d}{dr}[r(\rho_f\alpha_f B_{rx} + \rho_s\alpha_s\beta_{rx})] = -(\rho_f\alpha_f + \rho_s\alpha_s)g - \frac{\partial p}{\partial x} + \frac{1}{r}\frac{d}{dr}[r(\alpha_f\tau_{rx} + \alpha_s\sigma_{rx} + s_{rx})] \tag{5}$$

In addition, it can be showed that [10] the axial pressure gradient is uniform throughout the suspension, i.e., it is independent of both x and r in fully developed flow. Integrating Eq. (5) over the cross-section leads to

$$-\frac{\partial p}{\partial x} = \rho_f g + (\rho_s - \rho_f)g\bar{\alpha}_s - \frac{2}{R}(\alpha_f\tau_{rx} + s_{rx})_w \tag{6}$$

where the last term in the RHS is evaluated at the wall.

2.2. The general asymptotic approach

The asymptotic approach is based on four assumptions:

(a) In the studied flow regimes, the average solids volumetric concentrations remain low enough such that, one can consider $\bar{\alpha}_s \ll 1$.
(b) In this range, all phase mean variables are *continuous functions* of the average concentration.
(c) In addition, within this range, at least limited intervals exist in which, all phase mean variables are *continuously differentiable functions* of the average concentration.
(d) Local solids concentration $\alpha_s(r)$ is a monotonically increasing function of average concentration $\bar{\alpha}_s$.

Besides, there is an implicit assumption related with the phase mean variables in the General equations, according to which, these variables can be considered as continuously differentiable functions of time and space coordinates, especially, in this case, with respect to the radial coordinate r. Assumption (a), together with the fully developed flow requirement, limits the range of validity of the theory, typically, to CFB risers. Indeed, in the practical operating conditions of this process, average solids concentrations seldom exceed 10% in volume. Assumptions (b) and (c) generalize an experimentally established fact, at least for variables such as local particle mass fluxes and axial pressure gradient. On the contrary, assumption (d) is a fully theoretical hypothesis. It can only be supported by the fact that no contrary experimental evidence has been found to date. Finally, throughout this analysis, the superficial gas velocity is assumed to remain constant, as well as, the composition of the circulating solids; the only operating parameter to be varied is the solids loading of the flow characterized by the average solids concentration $\bar{\alpha}_s$.

Let us now consider an average concentration interval referred to as K. Within this interval, *reference flow conditions* will be defined by an average concentration $\bar{\alpha}_s^R$. Provided that, assumption (c) is valid over interval K, any generic fluid phase variable $\alpha_f\psi_f$ evaluated for an average concentration $\bar{\alpha}_s$, can be expressed using a Taylor series development such as

$$\alpha_f\psi_f = (\alpha_f\psi_f)^R + (\bar{\alpha}_s - \bar{\alpha}_s^R)\psi_f^K + O(\bar{\alpha}_s^2) \tag{7}$$

where the first term on the RHS represents $\alpha_f\psi_f$ evaluated under reference flow conditions. The second term is the first order term of the development; therefore, ψ_f^K which is a function of r depends on the superficial gas velocity, but is independent of $\bar{\alpha}_s$. Finally, $O(\bar{\alpha}_s^2)$ represents second and higher order terms, which can be neglected according to assumption (a). Similarly, for any solids phase variable one obtains

$$\alpha_s\psi_s = (\alpha_s\psi_s)^R + (\bar{\alpha}_s - \bar{\alpha}_s^R)\psi_s^K + O(\bar{\alpha}_s^2) \tag{8}$$

and especially, for local particle concentration

$$\alpha_s(r) = (\alpha_s)^R + (\bar{\alpha}_s - \bar{\alpha}_s^R)f^K(r) + O(\bar{\alpha}_s^2) \tag{9}$$

The corresponding development of the local probability of presence of the fluid α_f can be deduced from Eqs. (9) and (3). In addition to the local phase presence probabilities and generic phase variables, the Momentum Equations contain three other terms: the gas–solids interaction force, the intergranular shear stress and the pressure gradient. These terms can also be developed in Taylor series over the same average concentration interval as

$$F_x = (F_x)^R + (\bar{\alpha}_s - \bar{\alpha}_s^R)F_x^K + O(\bar{\alpha}_s^2) \tag{10}$$

$$s_{rx} = (s_{rx})^R + (\bar{\alpha}_s - \bar{\alpha}_s^R)s_{rx}^K + O(\bar{\alpha}_s^2) \tag{11}$$

$$-\frac{\partial p}{\partial x} = (G)^R + (\bar{\alpha}_s - \bar{\alpha}_s^R)G^K + O(\bar{\alpha}_s^2) \tag{12}$$

In all these Taylor series developments, the coefficients of the first order terms identified with a K superscript, are

independent of $\bar{\alpha}_s$ and, therefore, are *invariant functions of* r (except G^K which is a constant) *over the average concentration interval* K. These functions depend, however, on the superficial gas velocity. Insofar as second and higher order terms can be neglected according to assumption (a), they represent the rate of variation of corresponding local variables with the solids loading of the suspension measured by the average particle concentration $\bar{\alpha}_s$.

Let us now, substitute for these truncated developments into the Momentum Equations (1), (2) and (5); subtracting through the same equations expressed for reference flow conditions, then, neglecting second and higher order terms, and finally, dividing through by $(\bar{\alpha}_s - \bar{\alpha}_s^R)$ lead, respectively, to the following forms:

$$\frac{1}{r}\frac{d}{dr}(r\rho_f B_{rx}^K) = f^K\rho_f g - f^K(G)^R + (\alpha_f)^R G^K - F_x^K + \frac{1}{r}\frac{d}{dr}(r\tau_{rx}^K) \quad (13)$$

$$\frac{1}{r}\frac{d}{dr}(r\rho_s \beta_{rx}^K) = -f^K\rho_s g + f^K(G)^R + (\alpha_s)^R G^K + F_x^K + \frac{1}{r}\frac{d}{dr}[r(\sigma_{rx}^K + s_{rx}^K)] \quad (14)$$

$$\frac{1}{r}\frac{d}{dr}[r(\rho_f B_{rx}^K + \rho_s \beta_{rx}^K)] = -f^K(\rho_s - \rho_f)g + G^K + \frac{1}{r}\frac{d}{dr}[r(\tau_{rx}^K + \sigma_{rx}^K + s_{rx}^K)] \quad (15)$$

All the terms of these three equations are independent of $\bar{\alpha}_s$, and both of three are valid throughout the average concentration range referred to as K. At the first glance, Eqs. (13) and (14) depend on the reference flow conditions chosen within the interval, through $(\alpha_f)^R$, $(\alpha_s)^R$ and $(G)^R$. But if we change the value of $\bar{\alpha}_s^R$ the changes undergone by these terms are of the same relative order of magnitude as the terms already neglected. Thus, they have to be considered as invariant over interval K. Consequently, Eqs. (13)–(15) are intrinsic equations for the average concentration range referred to as K; they govern the radial distribution of the *rate of variation functions* associated with the local variables throughout K.

In other words, insofar as all local variables are continuously differentiable functions of average solids concentration throughout interval K, a unique set of rate of variation functions governed by Eqs. (13)–(15), define the evolution of local flow variables with solids loading, at a constant superficial gas velocity, throughout K. This is typically the kind of situation allowing to refer to interval K as harboring a consistent *flow regime*. Therefore, *the asymptotic approach provides a criterion* to decide if any range of solids loading can be considered as a specific flow regime for a fully developed gas–solids suspension. As the scope of this analysis is limited to fully developed suspension flow with moderate solids concentration as required by assumption (a), the only criterion is the validity of assumption (c).

3. The Similar Profiles Regime

3.1. Dilute phase flow

Let us now consider the range of very low solids loadings. Starting with a dilute suspension and progressively reducing solids loading to zero such that $\bar{\alpha}_s$ tends toward zero, while the superficial gas velocity is maintained constant, will lead to an unladen fluid flow. Indeed, as the local α_s is necessarily positive or zero, $\bar{\alpha}_s \to 0$ will result in $\alpha_s(r) \equiv 0$ throughout the cross-section. Besides, according to assumption (b), all local fluid phase variables will tend toward their expressions for the unladen gas flow, while, solids phase variables will identically, vanish.

Consequently, if $\bar{\alpha}_s^R = 0$ is taken as the reference flow conditions, one has

$$(\alpha_f\psi_f)^R = (\alpha_f\psi_f)^0 \equiv \psi_f^0 \quad (16)$$

$$(\alpha_s\psi_s)^R = (\alpha_s\psi_s)^0 \equiv 0 \quad (17)$$

$$(\alpha_s)^R = (\alpha_s)^0 \equiv 0 \quad (18)$$

Eqs. (7)–(9) will then, take the following form:

$$\alpha_f\psi_f = \psi_f^0 + \bar{\alpha}_s\psi_f^1 \quad (19)$$

$$\alpha_s\psi_s = \bar{\alpha}_s\psi_s^1 \quad (20)$$

$$\alpha_s(r) = \bar{\alpha}_s f^1(r) \quad (21)$$

where the 0 superscript is used to identify the variables of the unladen gas flow, and where the 1 superscript indicates the rate of variation functions associated with the local variables of the suspension, for this dilute phase flow. In these MacLaurin series developments, second and higher order terms have been omitted according to assumption (a). The generic form of Eq. (19) applies to all fluid phase variables, and also to the pressure gradient, while, Eq. (20) describes the variations of all solids phase variables including the gas–solids interaction force F_x and the intergranular stress s_{rx}, as both should vanish in unladen gas flow.

Provided that an appropriate solids loading interval exists, over which local phase variables remain continuously differentiable functions of average solids concentration, Eqs. (19)–(21) define a flow regime expected to occur under dilute phase flow conditions. In addition, Eqs. (20) and (21) define the radial profiles of solids phase variables as self-similar. Therefore, this dilute phase flow regime has been called the *Similar Profiles Regime* [10,12]. The radial profiles of solids phase variables should keep their self-similarity property regardless of the superficial gas velocity. Nevertheless, the shape of the profiles, i.e., the rate of variation functions such as $f^1(r)$ and $\psi_s^1(r)$ or $\psi_f^1(r)$ are expected to change when the gas velocity is changed.

The effective existence of this Similar Profiles Regime (SPR) has been confirmed by several experimental investigations. This will be discussed in the last section of this paper. However, given the limited number of reliable measuring

techniques, comparison was mainly performed for the pressure drop law, average solids velocity and particle mass flux profiles. Let us explicit the corresponding laws predicted by this theory.

The general form of the variations of unit pressure drop with average concentration, in the SPR, can be deduced from Eq. (12):

$$-\frac{\partial p}{\partial x} = (G)^0 + \bar{\alpha}_s G^1 \tag{22}$$

where $(G)^0$ stands for the pressure gradient of unladen gas flow for the same superficial velocity. Now, if we consider local solids velocity, Eq. (20) applies with $\psi_s = V_x$. Thus, one obtains

$$\alpha_s V_x = \bar{\alpha}_s V_x^1 \tag{23}$$

where V_x^1 is a function of radial coordinate and superficial gas velocity, but is independent of average solids concentration. The average solids velocity $\overline{V}$ is generally defined by

$$\bar{\alpha}_s \bar{V} = \frac{1}{A}\int_A \alpha_s V_x \, \mathrm{d}A \tag{24}$$

In the SPR, it is then, equal to the cross-sectional average of V_x^1. Given that the latter should be invariant when solids loading changes, *average solids velocity should remain constant* in the Similar Profiles Regime, and only depend on gas velocity. Finally, the RHS of Eq. (23) multiplied by ρ_s represents the local net particle mass flux in the axial direction. The average solids mass flux is defined by

$$\bar{\phi}_s = \frac{1}{A}\int_A \rho_s \alpha_s V_x \, \mathrm{d}A \tag{25}$$

Combining with Eq. (23) leads to

$$\phi_s(r) = \bar{\phi}_s \Lambda^1(r; U) \tag{26}$$

according to which, particle mass flux profiles should be self-similar. $\Lambda^1(r; U)$ is a function of radial distance and superficial gas velocity, to be determined experimentally.

Indeed, the analysis performed here can only show the general properties of the laws governing the variations of flow variables with solids loading, but is unable to predict the actual shape of the radial profiles, not even as a function of gas velocity.

3.2. The upper limit of the Similar Profiles Regime

Let us recall that Eqs. (19)–(21) are the limiting forms of Taylor series developments, asymptotically valid as $\bar{\alpha}_s \to 0$. Therefore, if the solids loading of the suspension, is further increased, the neglected second order terms are likely to progressively change the slope of the curves describing the variations of local variables with average concentration. Except, if there is an upper limit to the concentration interval over which local variables are continuously differentiable functions of $\bar{\alpha}_s$.

In order to examine the possibility of such an upper limit, let us now examine how local fluid phase variables are expected to change with *local* particle concentration, in dilute phase flow. According to Eq. (19), for very low particle loading, the fluid phase variables of the suspension depart weakly from their values in unladen gas flow; in addition, comparison with Eq. (21) suggests that the local perturbation of the unladen gas flow field is *proportional to local particle concentration*:

$$\alpha_f \psi_f - \psi_f^0 = \alpha_s \frac{\psi_f^1}{f^1} = \alpha_s \tilde{\psi}_f^1 \tag{27}$$

Now, let us consider the flow about a particle in such conditions. As it is well known from one-phase fluid mechanics, it significantly differs from "outer flow" only in a limited volume, namely, the boundary layer and the wake. Outside this "perturbated flow volume", local variables are essentially equal to those of the "outer flow". In the present case, the axial velocity component, for instance, is essentially equal to U_x^0. Besides, in the "perturbated flow volume", local velocity depends upon the slip velocity of the particle. Let u_x denote this local velocity, on the average. Therefore, the phase mean velocity (i.e., the expected value) U_x will be a combination of these two contributions. In addition, according to the similarity rules of one-phase fluid mechanics, the "perturbated volume" is proportional to the volume of the particle. Therefore, u_x will contribute to U_x in a volume fraction equal to $(k\alpha_s)$, while the unperturbated flow velocity will contribute in the complementary volume $(1 - k\alpha_s)$. Thus, one has

$$U_x = (1 - k\alpha_s)U_x^0 + k\alpha_s u_x \tag{28}$$

From an ensemble averaging point of view, $(k\alpha_s)$ and $(1 - k\alpha_s)$ are the respective probabilities to find the local velocity equal to, either u_x or U_x^0. A similar expression can be found for the velocity cofluctuations term B_{rx} (as well as, for other fluid phase variables); indeed, if b_{rx} denotes the average cofluctuation in the "perturbated volume", one has

$$B_{rx} = (1 - k\alpha_s)B_{rx}^0 + k\alpha_s b_{rx} \tag{29}$$

where B_{rx}^0 represents the turbulence of unladen gas flow. Obviously, Eqs. (28) and (29) are consistent with the general form (27). Nevertheless, these two expressions are valid, *if and only if*, $k\alpha_s < 1 - \alpha_s$, i.e., if the "perturbated flow volumes" do not overlap.

Consequently, insofar as Eqs. (28) and (29) can be considered as the physical justification of the general forms (27) and (19), one should contemplate that, all these forms could become invalid beyond a critical concentration α_s^* defined by

$$(k + 1)\alpha_s^* = 1 \tag{30}$$

Indeed, as soon as α_s reaches this critical value, the rate of variation of the fluid phase variables with local concentration is expected to change. Therefore, even if Eq. (21) describing the relationship between local concentration α_s and

average concentration, remains valid beyond α_s^*, *local fluid phase variables are no longer continuously differentiable functions of* $\bar{\alpha}_s$ *over a range containing* α_s^*. Consequently, α_s^* determine the upper limit of the Similar Profiles Regime.

However, the mechanism identified as being responsible for this upper bound is a *local* one, and α_s^* is a critical value for *local* concentration. When $\bar{\alpha}_s$ is progressively increased from zero, the local concentration will reach its critical value α_s^* at a radial position r^* in the cross-section, where particle concentration is maximum in the Similar Profiles Regime. According to Eq. (21), this will occur for an average concentration $\bar{\alpha}_s^*$ such that

$$\alpha_s^* = \bar{\alpha}_s^* f^1(r^*) \tag{31}$$

Therefore, in terms of average concentration, the Similar Profiles Regime would occur in a range $[0; \bar{\alpha}_s^*]$. Besides, α_s^* is determined by k which is a characteristics of the relative flow about a particle. Thus, it mainly depends on fluid and particle properties. But as the shape of concentration profiles in the Similar Profile Regime is likely to depend on gas velocity, $\bar{\alpha}_s^*$ is expected to be a function of superficial gas velocity.

4. The Transition Regime

4.1. Gradual transition

If the concentration profiles in the SPR were uniform throughout the cross-section, one would have $\bar{\alpha}_s^* = \alpha_s^*$. In other words, the change from Eqs. (28) and (29) to another set of laws of variation with local concentration, would occur simultaneously for the whole cross-section. However, concentration profiles are not expected to be uniform, even in the SPR, at least on the basis of the few available experimental results. Thus, for the *average* critical concentration $\bar{\alpha}_s^*$, $\alpha_s(r)$ will be lower than α_s^* everywhere in the cross-section except at $r = r^*$. If the solids loading is gradually increased, $\alpha_s(r)$ will increase everywhere throughout the flow, according to assumption (d), and the local critical conditions will be reached and overstepped in an larger and larger part of the cross-section. Let r^{**} denote the radial position where the local concentration will reach the critical value α_s^* at the latest, i.e., when $\bar{\alpha}_s = \bar{\alpha}_s^{**}$. Then, the average concentration range $[\bar{\alpha}_s^*; \bar{\alpha}_s^{**}]$ will correspond to the solids loading interval through which local transition progressively takes place throughout the cross-section. This range will be called the transition range and the above interval referred to as T.

As showed above, the flow structure of the SPR cannot hold in this range; in addition, beyond the upper bound of interval T, a new flow regime is expected to occur, which will be called below, the Dense Phase Flow Regime. Let us now examine the expected properties of the flow field, in between, i.e. over interval T.

All along this average concentration range, the relationship between local flow variables and local concentration, will still, be described by Eqs. (28) and (29) in the part of the cross-section where $\alpha_s(r) < \alpha_s^*$, while in the remaining part, the magnitude of which will increase with $\bar{\alpha}_s$, new local laws will apply. Let us, respectively, call "sub-critical flow region" and "super-critical flow region" these two parts.

Let us denote $c(r)$ the average concentration for which, the local concentration at a given radial distance r reaches the critical value α_s^*. Thus, $c(r)$ defines an implicit function of r through the following equation:

$$\alpha_s(r; c) = \alpha_s^* \tag{32}$$

Given that, α_s is assumed to be a continuous function of average concentration and a continuously differentiable function of radial distance, $c(r)$ would be a continuous function of r. Therefore, interval T is a range of solids loading over which a *gradual transition* occurs: the flow structure of the Similar Profiles Regime, *progressively and continuously* changes into that of dense phase flow, as overall solids loading is increased.

4.2. Flow structure

According to assumption (b), $\alpha_s(r; \bar{\alpha}_s)$ is a continuous function of average concentration, but not necessarily, a *continuously differentiable* function of that variable all over interval T. Nevertheless, its derivative with respect to $\bar{\alpha}_s$ cannot be discontinuous throughout the interval, otherwise, assumption (b) cannot remain valid. Therefore, interval T bears only a limited number of discrete points of discontinuity for that derivative. It is necessarily discontinuous for $\bar{\alpha}_s = \bar{\alpha}_s^*$ and $\bar{\alpha}_s = \bar{\alpha}_s^{**}$. In addition, the mechanism of progressive substitution described above, which closes up the local sub-critical flow conditions when the "perturbated flow volumes" overlap, suggests that such a discontinuity should also occur, at a given radial distance r, for $\alpha_s(r) = \alpha_s^*$, thus, for $\bar{\alpha}_s = c(r)$.

Therefore, let us assume that, the variations of local concentration with average concentration, are governed by two different laws depending on whether local flow conditions are sub-critical or super-critical:

$$\alpha_s^-(r; \bar{\alpha}_s) = \alpha_s^* + [\bar{\alpha}_s - c(r)] f^-(r; U) \tag{33}$$

$$\alpha_s^+(r; \bar{\alpha}_s) = \alpha_s^* + [\bar{\alpha}_s - c(r)] f^+(r; U) \tag{34}$$

In these equations, which express truncated Taylor series developments, the second and higher order terms have been neglected in accordance with assumption (a). In addition, the $(-)$ superscript has been used for sub-critical flow variables while, the $(+)$ superscript identifies the super-critical flow variables. Local concentration is expected to be a continuously differentiable function of radial distance, regardless of overall or local flow conditions. Therefore, $f^-(r)$, $f^+(r)$ and $c(r)$ should be alike. In addition, the radial derivative of $\alpha_s(r)$ should remain continuous throughout interval T, especially for $\bar{\alpha}_s = c(r)$. According to Eqs. (33) and (34), this

radial derivative is twofold:

$$\frac{d\alpha_s^-}{dr} = [\bar{\alpha}_s - c(r)]\frac{df^-}{dr} - f^-(r)\frac{dc}{dr} \quad (35)$$

$$\frac{d\alpha_s^+}{dr} = [\bar{\alpha}_s - c(r)]\frac{df^+}{dr} - f^+(r)\frac{dc}{dr} \quad (36)$$

Thus, provided that $c(r)$ is continuously differentiable, the continuity requirement for local critical conditions requires

$$f^-(r;U) = f^+(r;U) = f^T(r;U) \quad (37)$$

Consequently, comparison with Eqs. (33) and (34) indicates that, the variations of local concentration with average concentration are, in fact, described by a *unique* law throughout interval T:

$$\alpha_s(r;\bar{\alpha}_s) = (\alpha_s)^* + [\bar{\alpha}_s - \bar{\alpha}_s^*]f^T(r;U) \quad (38)$$

A similar mathematical argument can be developed for any other phase mean variable, either $\alpha_f\psi_f$ or $\alpha_s\psi_s$ to show that its variations with average concentration, are governed by a unique rate of variation function, either ψ_f^T or ψ_s^T all over interval T:

$$\alpha_f\psi_f = (\alpha_f\psi_f)^* + [\bar{\alpha}_s - \bar{\alpha}_s^*]\psi_f^T \quad (39)$$

$$\alpha_s\psi_s = (\alpha_s\psi_s)^* + [\bar{\alpha}_s - \bar{\alpha}_s^*]\psi_s^T \quad (40)$$

Again, there is a necessary condition for the validity of these equations: the function $c(r)$ should be a continuously differentiable function of the radial coordinate.

Eqs. (38)–(40) are of the same form as (7)–(9). Consequently, they define interval $T = [\bar{\alpha}_s^*; \bar{\alpha}_s^{**}]$ as a concentration interval over which, the variations of the local flow variables, with solids loading, are governed by a unique set of asymptotic laws making up a consistent flow regime. As this is a range over which local critical transition gradually occurs throughout the cross-section, it will be called the *Transition Regime*. It is characterized by affine laws of variation (in continuity with those of the SPR) of *all* local variables with average concentration.

Indeed, for the axial pressure gradient one obtains

$$-\frac{\partial p}{\partial x} = -\left(\frac{\partial p}{\partial x}\right)^* + [\bar{\alpha}_s - \bar{\alpha}_s^*]G^T \quad (41)$$

For the axial mass flux profiles, combining Eqs. (25) and (40) one can also find an affine law of variation:

$$\phi_s(r) = (\phi_s)^* + [\bar{\phi}_s - \bar{\phi}_s^*]\Lambda^T(r;U) \quad (42)$$

In addition, it can be easily shown that, in the Transition Regime, local as well as, average solids velocities become functions of average concentration, unlike the behavior observed in the SPR.

However, all these conclusions are valid only if $c(r)$ is a continuously differentiable function. In order to ascertain this property, let us note once, that the derivative of $c(r)$ cannot be discontinuous throughout the cross-section. It can only exhibit a discontinuity at a limited number of discrete radial positions. These are r^* and r^{**}. However, a possible discontinuity of the derivative at these points does not invalidate the previous conclusions. Indeed, the continuity of the derivative is required for the use of Eqs. (33)–(36). But for $r = r^*$, sub-critical flow conditions do not exist within the range of the Transition Regime, as for the super-critical flow conditions at $r = r^{**}$, alike. Therefore, derivability at these singular points is not required. Besides, if the existence of other points of discontinuity is to be suspected, $f^-(r)$ and $f^+(r)$ are expected to be different at these points. Since, these are isolated singular points, the necessary continuity of local concentration, as a function of radial distance, will impose the continuity of the rate of variation functions. In other words, if $r^\#$ denote such a radial distance, one should have

$$f^-(r^\#) = f^+(r^\#) = f^T(r^\#) \quad (43)$$

which implies that the general conclusion summarized by Eq. (37) remains valid even for these singular points. The conclusions derived in this section are, therefore, valid for the whole cross-section.

Consequently, as soon as the average concentration exceeds the critical value $\bar{\alpha}_s^*$, the Similar Profiles Regime will end, and the Transition Regime will take place. From a practical point of view, these two regimes will be different, if and only if, the rate of variation functions of the two regimes, are different. To ascertain this point, let us express the local critical concentration using Eq. (38):

$$\alpha_s^* = (\alpha_s)^* + [c(r) - \bar{\alpha}_s^*]f^T(r) \quad (44)$$

α_s^* can be obtained from Eq. (21). Combining these two equations leads to

$$f^T(r) - f^1(r) = \frac{\alpha_s^* - c(r)f^1(r)}{c(r) - \bar{\alpha}_s^*} \quad (45)$$

The numerator of the fraction in the RHS of this equation, only vanishes for $r = r^*$. Therefore, $f^T(r)$ and $f^1(r)$ are different throughout the cross-section, except, perhaps at $r = r^*$. At this particular radial position, the denominator simultaneously vanishes; the two rate of variation functions, thus, can be different even in r^*.

5. Dense Phase Flow Regime

Throughout the Similar Profiles Regime, solids phase variables are governed by Eqs. (20) and (21). Consequently, local solids velocity, for instance, remains constant, at a given radial position, and equal to the value it would assume for an isolated particle fed into the unladen gas stream, regardless of solids concentration. The *relative* radial distribution of the particles, alike, remain unchanged throughout the regime. In other words, on the average, the flow field of the particles is determined by the unladen gas flow field, while, overall particle loading, acts as a scale factor. According to this picture, one would expect, that the overall

solids loading could be increased, without any change in the properties of the particles flow field, as far as a *saturation* would occur in terms of local particle concentration, at least, at a particular radial position. It can be easily imagined that such a saturation would be the maximum concentration possible for the particles, i.e., for instance, the packed bed or, dense phase fluidized bed concentration.

We showed that, a saturation indeed occurs, which is not due, however, to particle packing limits but, to the effect of the presence of the particles on gas flow field. The gradual substitution, proportional to local particle concentration, of solids-dependent flow variables, for unladen flow variables, as described by Eqs. (29) and (30), imposes its intrinsic limit: the disappearance of any trace of unladen gas flow structure, at a given radial position, due to the overlapping of "perturbated flow volumes". As soon as the conditions for such a saturation occur, at any radial position in the cross-section, the relationship between local particle concentration and overall solids loading happens to change. The SPR ends up, to leave the place to the specific flow structure of the Transition Regime.

The saturation under consideration, however, is not a concentration which cannot be exceeded. It only results, in places where local saturation conditions are fulfilled, in solids variables independent of *local* unladen gas flow variables, but determined by a solids-dependent fluid flow structure. Throughout the Transition Regime, "saturated" and "unsaturated" flow conditions (which have been, respectively, termed as super-critical and sub-critical flow conditions) coexist over the cross-section. The requirements of this coexistence, shape the flow structure of the Transition Regime.

Obviously, beyond $\bar{\alpha}_s^{**}$, the complete disappearance of sub-critical flow conditions will require a new change in the relationships between local variables and average concentration. Therefore, a new flow regime will take place, which will extend as far as these relationships can be described by functions continuously differentiable with respect to $\bar{\alpha}_s$, i.e., unless a new type of saturation occurs. Tentatively, this regime will called the *Dense Phase Flow Regime* (DPR).

As far as the second and higher order terms can be neglected, this regime can be characterized by truncated Taylor series developments similar to Eqs. (7)–(9):

$$\alpha_f \psi_f = (\alpha_f \psi_f)^{**} + [\bar{\alpha}_s - \bar{\alpha}_s^{**}]\psi_f^D \tag{46}$$

$$\alpha_s \psi_s = (\alpha_s \psi_s)^{**} + [\bar{\alpha}_s - \bar{\alpha}_s^{**}]\psi_s^D \tag{47}$$

$$\alpha_s(r) = (\alpha_s)^{**} + [\bar{\alpha}_s - \bar{\alpha}_s^{**}] f^D(r; U) \tag{48}$$

and, in particular, for the unit pressure drop, and, the local solids mass fluxes, respectively:

$$-\frac{\partial p}{\partial x} = -\left(\frac{\partial p}{\partial x}\right)^{**} + [\bar{\alpha}_s - \bar{\alpha}_s^{**}]G^D \tag{49}$$

$$\phi_s(r) = (\phi_s)^{**} + [\bar{\phi}_s - \bar{\phi}_s^{**}]\Lambda^D(r; U) \tag{50}$$

Obviously, the DPR rate of variation functions identified with the (D) superscript, will differ from those of the Transition Regime.

The search of the conditions under which the DPR is expected to end up, is out of the scope of this paper. The only observation, which can be inferred, is that if, with increasing solids loading, the second and higher order terms become no longer negligible, Eqs. (46)–(50) will represent the initial trends of variation in the DPR, i.e., the equation of the tangent to the plot of the corresponding curve, for $\bar{\alpha}_s = \bar{\alpha}_s^{**}$.

6. Comparison with experimental results

During the last two decades, a lot of experimental work has been devoted to investigating flow regime and flow structure characteristics in vertical fully developed flow, especially, in CFB risers. Their results will shortly be analyzed, here in order to be compared to our theoretical predictions.

Through a careful series of experiments on dilute phase suspensions Muzyka et al. [15,16] was the first author to confirm that the pressure gradient of the suspension was, indeed, systematically described by Eq. (22), as predicted for the Similar Profiles Regime as can be seen in Fig. 1. His experiments have been carried out in a 20 mm ID stainless steel pipe, using two different particle size distributions of sand (172, 249 μm) and glass beads (63 μm) suspended in atmospheric air. His results show the rate of variation factor G^1 as being a linear function of superficial gas velocity, as can be predicted using Eq. (6) and modeling particle-wall collisions. In addition, Muzyka showed that the average solids velocity is independent of solids concentration, and, is a linear function of superficial gas velocity in the 1.5–10 m/s range. The average slip velocity was found essentially equal to the terminal velocity of the average particle, for the three solids.

Analyzing their average solids flux vs. average solids concentration plots, Monceaux et al. [17,18] reported the systematic existence of an abrupt change in the slope of the linear trends of variation, for different levels of superficial gas velocity (2–6 m/s), thus, suggesting a regime transition. Their experiments were carried out in a 144 mm ID plexiglass CFB-riser column in which, 60 μm FCC-catalyst particles were suspended in atmospheric air. They observed essentially self-similar particle mass flux profiles in the first regime (dilute phase flow) while, the profiles deformed with solids loading in the second regime, exhibiting a significant downflow near the wall.

With the help of his experiments, performed in the same installation as Muzyka, using a 210 μm sand, Mok [6,7,19] reported three flow regimes occurring, at a constant superficial gas velocity, when solids loading is gradually increased. Fig. 2 shows for $\bar{\phi}_s$ vs. $\bar{\alpha}_s$ the characteristic broken line behavior predicted in present work, suggesting an identification of the three linear regression lines with the analyzed regimes. A similar trend of variation is also exhibited by his pressure drop vs. $\bar{\alpha}_s$ data in agreement with Eqs. (22),

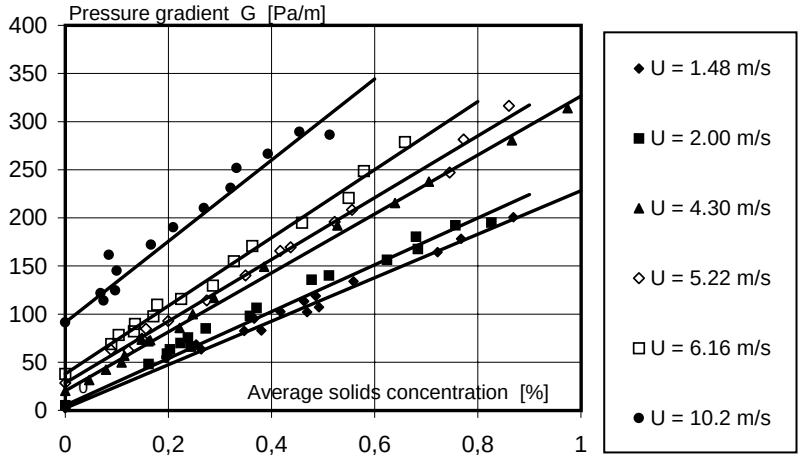

Fig. 1. Pressure drop in dilute phase flow of vertical gas–solids suspensions after Muzyka [16]. Regression lines confirm the linear trend of variation with average concentration $\bar{\alpha}_s$ at constant gas velocity U as predicted by Eq. (22).

(41) and (49). In addition, the slip velocity remains invariant and essentially equal to the terminal velocity of the average particle, in the first regime identifiable with the SPR. It substantially increases with concentration in the second, which probably corresponds to the Transition Regime, and, essentially stabilizes in dense phase flow.

Ginestet et al. [20,21] investigating pneumatic transport in a 31.8 mm ID pipe, either vertical, or inclined, and plotting their data in the same way, also reported the two first regimes with their characteristics derived here, for 186 μm sand and 571 μm glass beads. The critical concentrations at which transition occurs are lower for an inclined pipe. However, with 2–3 mm coleseed, the abrupt changes of slope are no longer obvious; rather, a progressive sharpening of the trend of variation is observed, e.g., in $\bar{\alpha}_s$ vs. $\bar{\phi}_s$ plots. This is probably due to the second and higher order terms, which could become non-negligible before the occurrence of the critical conditions required for the regime transition.

Working with the same installation as Monceaux et al. [17,18], Bodelin [22–24] showed that they missed the authentic SPR which occur for 60 μm FCC-catalyst particles at average concentrations lower than about 0.2–0.4%. He also investigated mass flux profiles for 198 μm sand and FCC-catalyst/sand mixtures. A typical plot of the trend of variation of local particle mass fluxes $\phi_s(r)$ for sand, with $(\rho_s\bar{\alpha}_s)$ at a constant gas velocity is shown in Fig. 3. Regression lines are in agreement with the trend of variation predicted by Eqs. (17) and (40). The same formal agreement has been observed with mixtures of solids differing both by their densities and their size distributions.

The same flow regimes, have been observed by Fabre et al. [25] in a 0.8 m × 1.2 m CFB-riser column operated using 260 μm sand particles. These authors report, however, a fourth linear portion in the broken line plots evoked above. This can be interpreted as the effect of the rectangular shape of the cross-section of the column. Indeed, as it is generally

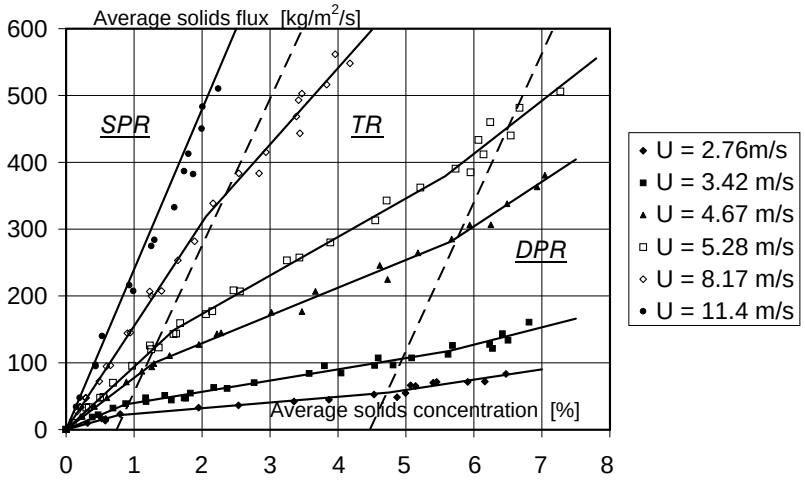

Fig. 2. Variations of average solids flux $\bar{\phi}_s$ with average concentration $\bar{\alpha}_s$ at constant velocities U, after Mok [7]. Regression lines exhibit the typical broken line behavior predicted in present work allowing flow regime identification. Dashed lines indicate the approximate bounds of the Transition Regime (TR).

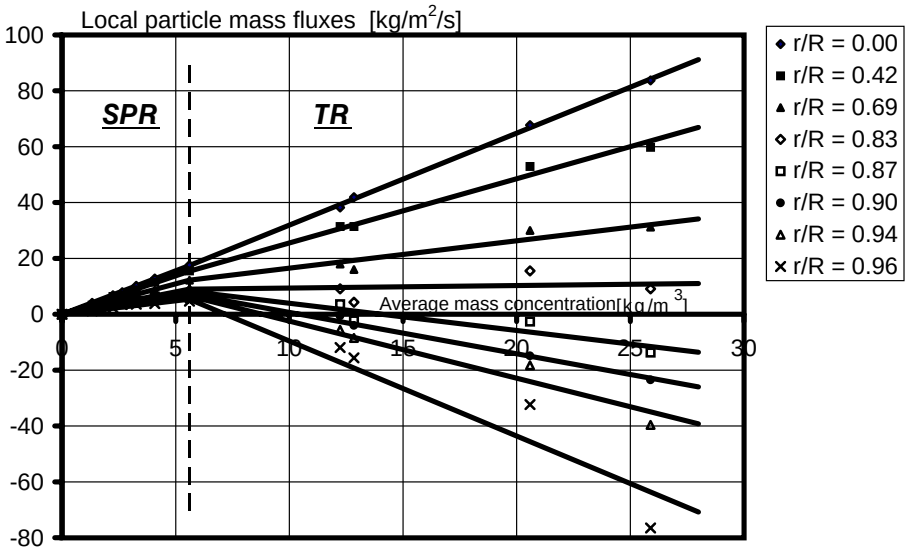

Fig. 3. Trend of variation of local particle mass fluxes $\phi_s(r)$ measured at different relative radial positions r/R, with average mass concentration ($\rho_s\bar{\alpha}_s$), after Bodelin [22]. Solids: 198 μm sand; $U = 4.4$ m/s. The dashed line indicates the onset of the Transition Regime (TR) for $\rho_s\bar{\alpha}_s = 5.6\,\mathrm{kg/m^3}$.

believed, the local concentration is expected to be maximum near the wall. Therefore, local transition should firstly occur near the wall, and then, progressively move toward the centerline. This progression remains axisymmetrical in a circular cross-section column, but local transition can reach the center, faster, along the short axis, than along the longer axis of a rectangular cross-section. Then, in the remaining sub-critical flow region, local transition will progress both from and toward the centerline. In addition, this argument could explain, why the average concentration sharply increases, in this range, for slight increments of average solids flux.

Finally, Motte et al. [26] with the same installation as Bodelin, confirmed the existence of the predicted flow regimes for particles mixes differing either by their size distributions or by their densities. An illustration is shown in Fig. 4. The three regimes can be clearly identified comparing the trends of variation with present predictions. The same regimes always occur in the same order. Nevertheless, the overall critical conditions $\bar{\alpha}_s^*$ and $\bar{\alpha}_s^{**}$, depend on the composition of the mixture: the finer the particles, the lower the critical concentrations. The effect of particle density, however, is less obvious.

Besides, the asymptotic analysis developed here, has been extended to temperature fields, in the Similar Profiles Regime, by Molodtsof and Muzyka [27]. Then, an explicit equation has been derived, for the variations of the wall-to-suspension heat transfer coefficient with solids

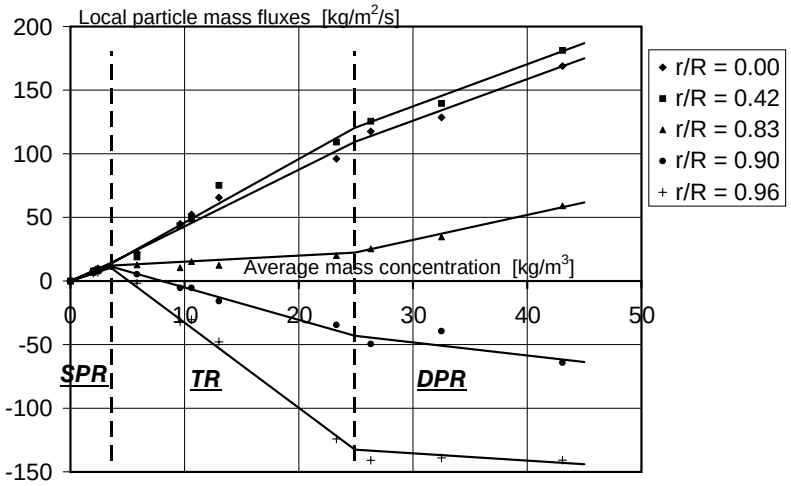

Fig. 4. Trend of variation of local particle mass fluxes $\phi_s(r)$ measured at different relative radial positions r/R, with average mass concentration ($\rho_1\bar{\alpha}_1 + \rho_2\bar{\alpha}_2$), after Motte [9]. Solids: a mix of 30% FCC-catalyst (1200 kg/m^3; 70 μm) and 70% iron ore (5200 kg/m^3; 83 μm); $U = 4.4$ m/s. The dashed lines indicate the bounds of the Transition Regime (TR).

loading, which predicts all previously observed trends, and, which has been found in excellent agreement with the heat transfer data reported by Muzyka [16]. In addition, Bentahar et al. [28] showed that, the sudden regime transition occurring for $\bar{\alpha}_s = \bar{\alpha}_s^*$ results in an abrupt change in the constants of the heat transfer coefficient equation.

7. Conclusions

An asymptotic analysis of the requirements of the general multiphase flow equations has been developed, for fully developed, vertical gas–solids suspensions. From this analysis the formal relationship between local flow variables and overall solids loading has been deduced. The examination of flow structure properties allowed the identification of three distinct flow regimes. The mechanism governing the hydrodynamic effect of local particle concentration, on local fluid phase variables, explains the regime changes, as well as the flow structure properties. The formal and qualitative predictions of this theoretical approach have been shown to be in excellent agreement with existing experimental results. These experimental data were obtained for particle diameters ranging from 40 μm to 1 mm, different solids densities, and even, for particle mixes, in risers the cross-sectional area of which range, from 3×10^{-4} to 1 m^2. Typical gas velocities were about 2–10 m/s. However, the analysis and its results, are valid for low and moderate solids loadings, i.e., for particle concentrations typically lower than 5–10% in volume. Consequently, the theory can be used as a general scheme for the prediction of trends, and the interpretation of the behavior of existing pilot-scale or even, commercial units.

References

[1] F.A. Zenz, Two-phase fluid–solid flow, Ind. Eng. Chem. 41 (1949) 2801–2806.
[2] L. Reh, Fluid bed processing, Chem. Eng. Progr. 67 (1971) 58–63.
[3] J. Yerushalmi, N.T. Cankurt, D. Geldart, B. Liss, Flow regimes in vertical gas–solid contact systems, AIChE Symp. Ser. 176 (74) (1978) 1–13.
[4] J.M. Matsen, Mechanisms of chocking and entrainment, Powder Technol. 32 (1982) 21–33.
[5] J.R. Grace, Contacting modes and behaviour classification of gas–solid and other two-phase suspensions, Can. J. Chem. Eng. 64 (1986) 353–362.
[6] S.L.K. Mok, Y. Molodtsof, J.F. Large, M.A. Bergougnou, Characterization of dilute and dense phase vertical upflow gas–solid transport based on average concentration and velocity data, Can. J. Chem. Eng. 67 (1989) 10–16.
[7] S.L.K. Mok, The study of hydrodynamic characteristics of vertical upflow gas–solids suspensions in the dilute and dense phase regimes, Ph.D. Thesis, University of Western Ontario, Canada, 1991.
[8] F. Berruti, J. Chaouki, L. Godfroy, T.S. Pugsley, G.S. Patience, Hydrodynamics of circulating fluidized bed risers: a review, Can. J. Chem. Eng. 73 (1995) 579–602.
[9] J. Motte, Etude du comportement hydrodynamique des mélanges multi-solides dans un lit fluidisé circulant, Thèse de Doctorat, Université de Technologie de Compiègne, France, 1996.
[10] Y. Molodtsof, Equations générales probabilistes des écoulements polyphasiques et applications aux mélanges gaz-solides, Thèse d'Etat, Université de Technologie de Compiègne, France, 1985.
[11] Y. Molodtsof, D.W. Muzyka, General probabilistic multiphase flow equations for analyzing gas–solids mixtures, Int. J. Eng. Fluid Mech. 2 (1989) 1–24.
[12] Y. Molodtsof, D.W. Muzyka, A similar profile regime in the vertical fully developed flow of gas–solids suspensions, Int. J. Multiphase Flow 17 (1991) 573–583.
[13] S.B. Savage, D.J. Jeffy, J. Fluid Mech. 110 (1980) 223–256.
[14] O. Simonin, P.L. Viollet, in: G.F. Hewitt, F. Mayinger, J.R. Riznic (Eds.), Phase–Interface Phenomena in Multiphase Flow, Hemisphere, Washington, DC, 1990, pp. 259–269.
[15] D.W. Muzyka, Y. Molodtsof, J.F. Large, M.A. Bergougnou, Application of probabilistic multiphase flow equations to dilute phase pneumatic transport, in: Proceedings of the 33rd Canadian Society Chemical Engineering Conference, Toronto, Canada, October 3–5, 1983.
[16] D.W. Muzyka, The use of probabilistic multiphase flow equations in the study of the hydrodynamics and heat transfer in gas–solids suspensions, Ph.D. Thesis, University of Western Ontario, London, Ont., Canada, 1985.
[17] L. Monceaux, M. Azzi, Y. Molodtsof, J.F. Large, Overall and local characterization of flow regimes in a circulating fluidized bed, in: P. Basu (Ed.), Circulating Fluidized Bed Technology, 1986, pp. 185–191.
[18] L. Monceaux, M. Azzi, Y. Molodtsof, J.F. Large, Particle mass flux profiles and flow regime characterization in a pilot-scale fast fluidized bed unit, in: Œstergaard and Sœrensen (Eds.), Fluidization V, 1986, pp. 337–44.
[19] S.L.K. Mok, Y. Molodtsof, J.F. Large, M.A. Bergougnou, Hydrodynamic characteristics of dilute phase flows in vertical pneumatic transport, in: Proceedings of the 37th Canadian Society Chemical Engineering Conference, Montréal, Canada, May 12–22, 1987.
[20] A. Ginestet, P. Guigon, J.F. Large, S. Sen Gupta, J.M. Beekmans, Hydrodynamics of a flowing gas–solids suspension in a tube at high angles of inclination, Can. J. Chem. Eng. 71 (1993) 177–182.
[21] A. Ginestet, P. Guigon, J.F. Large, J.M. Beekmans, Further studies on flowing gas–solids suspensions in a tube at highangles of inclination, Can. J. Chem. Eng. 72 (1994) 582–587.
[22] P. Bodelin, Caractérisation de la structure d'écoulement dans la colonne d'un lit fluidisé circulant et application aux mélanges de particules, Thèse de Doctorat, Université de Technologie de Compiègne, France, 1994.
[23] P. Bodelin, Y. Molodtsof, A. Delebarre, Flow regimes and flow structure in a CFB, in: A. Avidan (Ed.), Circulating Fluidized Bed Technology IV, AIChE, 1994, pp. 118–122.
[24] P. Bodelin, Y. Molodtsof, A. Delebarre, Behaviour of single solids and their binary mixtures in a circulating fluidized bed, in: J.F. Large, C. Laguérie (Eds.), Fluidization VIII, Engineering Foundation, 1995, pp. 271–280.
[25] A. Fabre, Y. Molodtsof, A. Koniuta, Flow structure characterization in a 1 sq. m. CFB, in: M. Kwauk, J. Li (Eds.), Circulating Fluidized Bed Technology V, Science Press, Beijing, 1997, pp. 645–651.
[26] J. Motte, Y. Molodtsof, A. Delebarre, Hydrodynamics and flow regimes in a CFB operated with multi-component mixtures, in: Fluidization IX, 1998.
[27] Y. Molodtsof, D.W. Muzyka, Wall to suspension heat transfer in the similar profiles regime, Int. J. Heat Mass Transf. 35 (1992) 2665–2673.
[28] F. Bentahar, Y. Molodtsof, J.F. Large, K. Alia, Heat transfer to vertically flowing dilute and dense phase gas–solids suspensions, AIChE Symp. Ser. 276 (86) (1990) 10–15.